

promoting access to White Rose research papers



Universities of Leeds, Sheffield and York
<http://eprints.whiterose.ac.uk/>

This is an author produced version of a paper published in **Nature Geoscience**

White Rose Research Online URL for this paper:

<http://eprints.whiterose.ac.uk/id/eprint/77809>

Paper:

Dobson, DP, Miyajima, N, Nestola, F, Alvaro, M, Casati, N, Liebske, C, Wood, IG and Walker, AM (2013) *Strong inheritance of texture between perovskite and post-perovskite in the D'' layer*. Nature Geoscience, 6. 575 - 578. ISSN 1752-0894

<http://dx.doi.org/10.1038/ngeo1844>

Strong texture inheritance between perovskite and post-perovskite in the D'' layer.

**David P. Dobson^{1,2}, Nobuyoshi Miyajima³, Fabrizio Nestola⁴, Matteo Alvaro⁴, Nicola Casati⁵,
Christian Liebske², Ian G Wood¹ and Andrew M. Walker⁶.**

¹*Department of Earth Sciences, University College London, Gower Street, London, WC1E 6BT, U.K.*

²*Institute for Geochemistry and Petrology, Clausiusstrasse 25, NW, ETH Zürich, CH-8092 Zürich, Switzerland*

³*Bayerisches Geoinstitut, Universität Bayreuth, D-95440, Bayreuth, Germany*

⁴*Department of Geosciences, University of Padua, Via Gradenigo 6, I-35131, Padova, Italy*

⁵*Paul Scherrer Institut, Swiss Light Source, 5232 Villigen PSI, Switzerland*

⁶*Department of Earth Sciences, Bristol University, Queens Road, Bristol, U.K.*

This is the archived post-print manuscript of a paper published online in Nature Geoscience on 16 June 2013. A typeset and copy-edited version can be found at <http://www.nature.com/ngeo/index.html> or by following this link <http://dx.doi.org/10.1038/ngeo1844> via the DOI. The paper should be cited as D. P. Dobson, N. Miyajima, F. Nestola, M. Alvaro, N. Casati, C. Liebske, I. G. Wood and A. M. Walker (2013) Strong texture inheritance between perovskite and post-perovskite in the D'' layer. Nature Geoscience vol.6 pp.576-578.

The main mineral in the lower mantle, magnesium-silicate perovskite, transforms into a high-pressure, post-perovskite, phase at pressures and temperatures corresponding to the D'' seismic discontinuity approximately 200 km above the core-mantle boundary^{1,2}. The strong elastic anisotropy of post-perovskite has been invoked to explain the observed seismic anisotropy and to infer flow in the D'' region, based on models of textured post-perovskite³⁻⁵. Such inferences rely on a knowledge of the mechanisms by which the post-perovskite can obtain texture. It is generally thought that seismic anisotropy in D'' is produced from lattice-preferred orientation generated during plastic deformation⁶⁻¹⁰; however, it is difficult to explain all of the observed seismic anisotropy in D'' using a single deformation mechanism in post-perovskite. Here we show that strong texture inheritance is possible during

transformation from perovskite to post-perovskite using a recently developed fluoride analogue system¹¹. If a similar transformation mechanism operates in the Earth, post-perovskite will inherit textures from deformed perovskite and vice versa as lower-mantle material passes into and out of regions of post-perovskite stability. This texture inheritance during the transition from post-perovskite to perovskite, combined with a single slip system in post-perovskite, can explain the seismic anisotropy of the lowermost mantle.

We compressed flux-grown single crystals of NaNiF_3 perovskite to 22 GPa and annealed them at 700 °C (within the post-perovskite stability field in this system; see supplementary methods) for 24 hours. The recovered crystals maintained their gross morphology but were cloudy in appearance. Single-crystal X-ray diffraction demonstrated that the perovskite had partially transformed to post-perovskite and that the c -axes of the two phases were parallel (for the **Pbnm** setting of the orthorhombic perovskite and the usual **C** face-centred description of the orthorhombic post-perovskite unit cell). Furthermore post-perovskite a -axes were either parallel to the perovskite b -axis or, more commonly, they were canted from it by 16.75 degrees (supplementary results), indicative of twinning on (110) in the post-perovskite with the composition plane containing the perovskite b -axis.

High-resolution TEM images of the partially transformed sample show the same relationship as the XRD measurements, with the normal to (110) in the post-perovskite, i.e. the vector $hh0$ in reciprocal space, parallel to [010] in the perovskite ($hh0010$) and 001001 (Figure 1). The electron diffraction pattern from this region shows a clear (110) twin relationship in the post-perovskite, with the composition plane between the twin domains closely sub-parallel to the perovskite **b***-reciprocal lattice vector (figure 1b). Figure 1c shows our interpretation of the X-ray and TEM data. Post-perovskite can be derived from perovskite by introducing stacking faults, along either of the (pseudocubic axial) directions which are diagonal to the orthorhombic setting, such that BX_6 octahedral units are edge-connected to the perovskite substrate layer. This results in a layered post-perovskite structure with sheets of BX_6 octahedra separated by layers of AX_6 polyhedra, with the c -axis of post-perovskite preserving the original perovskite c -axis. The

C-centring of post-perovskite requires that its a and b unit cell axes are canted to the perovskite unit cell with $(110)_{\text{PPV}}$ perpendicular to $[010]_{\text{PV}}$. Domains of post-perovskite derived from symmetrically equivalent octahedra in the perovskite structure can then grow in a (110) normal twinning relationship with the b -axis of the host perovskite parallel to the twin axis.

A martensitic transformation mechanism which produces these topotactic relations was previously inferred from the results of ab initio metadynamics calculations¹² but this is the first time that topotaxy has been observed experimentally between perovskite and post-perovskite. Our observed topotaxy in the recoverable fluoride system is corroborated by a study in which polytypes of post-perovskite were produced from Al-bearing MgSiO_3 perovskite (ref 13). These polytypes have kinked post-perovskite structures which are effectively ordered (110) twins, suggesting that this twin mechanism is activated in aluminous-post-perovskite MgSiO_3 during transformation from perovskite starting material. The observed topotaxy is further supported in the natural system by the observation that deformation experiments in post-perovskite MgGeO_3 and MgSiO_3 initially show $\{110\}$ -slip textures immediately after transformation from perovskite which subsequently evolve to the true post-perovskite deformation texture¹⁰. This $\{110\}$ texture is produced since perovskite deforms by slip on (010) ^{14,15} and subsequent transformation converts $(010)_{\text{PV}}$ into $(110)_{\text{PPV}}$, resulting in an apparent $\{110\}$ post-perovskite deformation texture. Given all of this evidence it seems very likely that the transformation mechanism observed here also operates in the silicate system, resulting in strong inherited textures as lower mantle material crosses into and out of the post-perovskite stability field in D'' , initially during downwelling of cold subducted material and then as D'' material warms up by conductive heating from the outer core¹⁶.

The majority of the mantle in D'' flows horizontally as cold downwellings force material along the core-mantle boundary (CMB) towards hotter regions of mantle upwelling. This shear deformation produces a lattice preferred orientation, and hence seismic anisotropy, in post-perovskite. The deformation mechanism of post-perovskite in D'' is still controversial, with different deformation experiments suggesting dominant slip on $\{110\}$ or (100) ^{6,8}, (010) ^{7,9} and, recently, (001) ¹⁷ planes. Global anisotropic

tomography^{18,19} yields models of the lowermost mantle with horizontally polarized shear waves with a higher velocity than vertically polarized shear waves in presumed cold regions such as the circum-Pacific. The opposite sense of anisotropy is found in locations expected to be hotter such as the central Pacific and African large low shear velocity provinces. Fitting these global observations using forward models of mantle deformation, requires slip on (010) or (100) to dominate²⁰. Conversely regional studies, where the seismic anisotropy is better constrained by crossing ray paths, find that slip on (001) fits the observed anisotropy best³. In addition, combined geodynamical and texture evolution models find that slip on (001), combined with textured MgO produces seismic anisotropy in D'' which is most like geophysical observations²¹. None of these studies, however, take account of the fact that perovskite is expected to become the stable phase of MgSiO₃ in hot regions of D'' (eg ref. 16). Here we suggest that the regional studies can be reconciled with the global observations if perovskite inherits texture from post-perovskite through the observed topotactic relations. To illustrate this we have performed viscoplastic self-consistent modelling²² of an (001) dominated slip system in post-perovskite to predict the texture generated during horizontal mantle flow in cold regions at the CMB (see supplementary information for details). We then transformed this texture using the observed topotaxy relations between perovskite and post-perovskite in order to predict the texture inherited by perovskite in hot regions of D''. Figure 2 shows the seismic anisotropy generated by horizontal simple shear in post perovskite and subsequent transformation to perovskite. The post-perovskite displays strong shear-wave anisotropy for horizontally propagating waves with horizontally polarised waves travelling faster than vertically polarised waves. The perovskite produced from this textured post-perovskite shows the opposite sense of anisotropy for horizontally propagating shear waves, consistent with global anisotropy tomography studies. We address the question of whether this 'transformation' texture will survive subsequent deformation in the perovskite stability field in figure 2 c, where the perovskite texture produced from the transformation has been subjected to the same shear strain again using the slip system of ref. 14 and the texture is not significantly altered. It is possible that perovskite in D'' will deform by diffusion creep; in this case, recent numerical simulations²³ have shown that textures can be preserved during diffusion creep, although they will be somewhat weakened.

The present interpretation reconciles the regional and global seismic studies whilst also being consistent with the positive Clapeyron slope of the transition between perovskite and post perovskite. It also raises the interesting possibility that studies which compare the shear-wave velocity with shear-wave anisotropy might be able to map out the extent of post-perovskite stability in D". In addition, the generation of texture in post-perovskite has been invoked as a means to produce a D" reflector even with gradual transformation from perovskite to post-perovskite²⁴. In a similar manner, perovskite which formed by transformation of post-perovskite will have a texture which varies strongly from that of perovskite in the overlying mantle which never entered the post-perovskite stability field. The resultant change in seismic anisotropy between these two regions of perovskite might explain the persistence of a D" reflector in the large, low-shear velocity provinces where post-perovskite is thought not to be stable.

Further work is required to confirm that the transformation mechanism observed here operates in the Earth. Martensitic transformation is enhanced compared to reconstructive transformation mechanisms by metastable overstep, which was large in the experiments and is likely to be small at the temperatures of D", and by shear deformation, which was zero in the experiments but certainly occurs in D". In addition, martensitic transformation under conditions of shear deformation is likely to have a further selectivity in the orientation of the daughter phase (ie both of the twin domains in the post-perovskite will not be equally developed), slightly modifying the textures which we predict here. This will not, however, significantly alter the conclusions since the difference in orientation between the two twin domains is small. Experiments are currently being performed to determine the strength of the selectivity during transformation in non-hydrostatic stress fields.

We have chosen to concentrate in this paper on the effect of topotaxy during the 'retrograde' transformation from post-perovskite to perovskite; however, similar effects will obtain during the 'prograde' reaction to post-perovskite. Since (010) planes are thought to be the weakest glide planes in perovskite^{14,15}, subducting slab material will generate a texture on entering D" with {110} post-perovskite planes parallel to the shear direction. Any transformation texture produced in this way should

subsequently be replaced by a true post-perovskite deformation texture. We caution strongly against interpreting observations of seismic anisotropy in D'' in terms of mantle flow without considering the transformation between perovskite and post-perovskite.

References.

1. Murakami, M., Hirose, K., Kawamura, K., Sata, N., Ohishi, Y. Post Perovskite Phase Transition in MgSiO₃. *Science* **304**, 855-858 (2004).
2. Oganov, A. R. and Ono, S. Theoretical and Experimental Evidence for a Post-Perovskite Phase of MgSiO₃ in Earth's D'' layer. *Nature* **430**, 445-448 (2004).
3. Nowacki, A., Wookey, J. & Kendall, J. M. Deformation of the lowermost mantle from seismic anisotropy *Nature* **467**, 1091-1906 (2010).
4. Garnero, E. J., and McNamara, A. K. Structure and dynamics of Earth's lower mantle, *Science* **320**, 626-628 (2008).
5. Wookey, J., and Kendall, J. M. Constraints on lowermost mantle mineralogy and fabric beneath Siberia from seismic anisotropy, *Earth Planet. Sci. Lett.* **275**, 32-42 (2008).
6. Merkel, S., Kubo, A., Miyagi, L., Speziale, S., Duffy, T. S., Mao, H. K. and Wenk, H. R. Plastic deformation of MgGeO₃ post-perovskite at lower mantle pressures, *Science* **311**, 644-646, (2006).
7. Yamazaki, D., Yoshino, T., Ohfuji, H., Ando, J. I. and Yoneda, A. Origin of seismic anisotropy in the D '' layer inferred from shear deformation experiments on postperovskite phase, *Earth Planet. Sci. Lett.* **252**, 372-378 (2006).
8. Merkel, S., McNamara, A. K., Kubo, A., Speziale, S., Miyagi, L., Meng, Y., Duffy, T. S. and Wenk, H. R. Deformation of (Mg,Fe)SiO₃ post-perovskite and D anisotropy, *Science* **316**, 1729-1732 (2007).
9. Walte, N., Heidelbach, F., Miyajima, N. and Frost, D. Texture development and TEM analysis of deformed CaIrO₃: Implications for the D '' layer at the core-mantle boundary, *Geophys. Res. Lett.* **34**, L08306 (2007).
10. Miyagi, L., Kanitpanyacharoen W., Stackhouse, S., Militzer, B. and Wenk, H. R. The enigma of post-perovskite anisotropy: deformation versus transformation textures *Phys. Chem. Mineral.* **38**, 665-678 (2011).

11. Dobson D. P., Hunt S. A., Lindsay-Scott, A. and Wood, I. G. Towards better analogues for MgSiO₃ post-perovskite: NaCoF₃ and NaNiF₃, two new recoverable post-perovskite phases. *Phys. Earth. Planet. Inter.* **189**, 171-175 (2011).
12. Oganov, A. R., Martonak, R., Laio, A., Raiteri, P. and Parrinello, M. Anisotropy of Earth's D'' layer and stacking faults in the MgSiO₃ post-perovskite phase, *Nature* **438**, 1142-1144 (2005).
13. Tschauner, O., Kiefer, B., Liu, H., Sinogeikin, S., Somayazulu, M. and Luo, S. N. Possible structural polymorphism in Al-bearing magnesium silicate post-perovskite. *Am. Mineral.* **93**, 533–539 (2008).
14. Carrez, Ph., Ferré, D. and Cordier, P. Peierls–Nabarro model for dislocations in MgSiO₃ post-perovskite calculated at 120 GPa from first principles, *Phil. Mag.* **87**, 3229-3247 (2007).
15. Mainprice, D., Tommasi, A., Ferré, D., Carrez, P. and Cordier, P. Predicted glide systems and crystal preferred orientations of polycrystalline silicate Mg-Perovskite at high pressure: Implications for the seismic anisotropy in the lower mantle. *Earth Planet. Sci. Lett.* **271**, 135–144 (2008).
16. Hernlund, J. W. Thomas, T. and Tackley, P. J. A doubling of the post-perovskite phase boundary and structure of the Earth's lowermost mantle. *Nature* **434**, 882-886 (2005).
17. Miyagi, L., Kanitpanyacharoen, W., Kaercher, P., Lee, K. K. M. and Wenk, H. R. Slip systems in MgSiO₃ postperovskite: implications for D'' anisotropy, *Science* **329**, 1636–1638 (2010).
18. Panning, M. and Romanowicz, B. A three-dimensional radially anisotropic model of shear velocity in the whole mantle. *Geophys. J. Int.* **167**, 361–379 (2006).
19. Kustowski, B., Ekström, G., and Dziewoński, A. Anisotropic shear-wave velocity structure of the Earth's mantle: a global model, *J. Geophys. Res.* **113**, B06306 (2008).
20. Walker, A. M., Forte, A. M. Wookey, J. Nowacki, A. and Kendall, J. M. Elastic anisotropy of D'' predicted from global models of mantle flow, *Geochem. Geophys. Geosyst.* **12**, Q10006 (2011).
21. Wenk, H. R., Cottaar, S., Tomé, C. N., McNamara, A. and Romanowicz, B. Deformation in the lowermost mantle: From polycrystal plasticity to seismic anisotropy. *Earth Planet. Sci. Lett.* **306**, 33–45 (2011).
22. Mainprice, D., A Fortran Program to Calculate Seismic Anisotropy from the Lattice Preferred Orientation of Minerals, *Computers & Geosciences* **16**, 385-393 (1990).
23. Wheeler, J. The preservation of seismic anisotropy in the Earth's mantle during diffusion creep. *Geophys. J. Int.* **178**, 1723-1732 (2009),
24. Ammann, M. W., Brodholt, J. P., Wookey, J. and Dobson, D. P. First Principles Constraints on Diffusion in Lower Mantle Minerals and a Weak D'' Layer. *Nature* **465**, 462-465 (2010).

Acknowledgements.

This work was supported by a Natural Environment Research Council grant to D.P.D. (ref J009520), and European Research Council starting grants to F.N. (ref 307312) and supporting A.M.W. (ref 240273).

Author contributions.

High-pressure experiments D.P.D. and C.L.; XRD experiments F.N., M.A., N.C. and D.P.D.; TEM experiments N.M.; crystallographic interpretation I.G.W. and D.P.D.; seismic anisotropy simulations A.M.W.

Additional information

Supplementary information accompanies this paper on www.nature.com/naturegeoscience. Reprints and permissions information is available online at <http://npg.nature.com/reprintsandpermissions>.

Correspondence and requests for materials should be addressed to D.P.D. d.dobson@ucl.ac.uk.

Figures

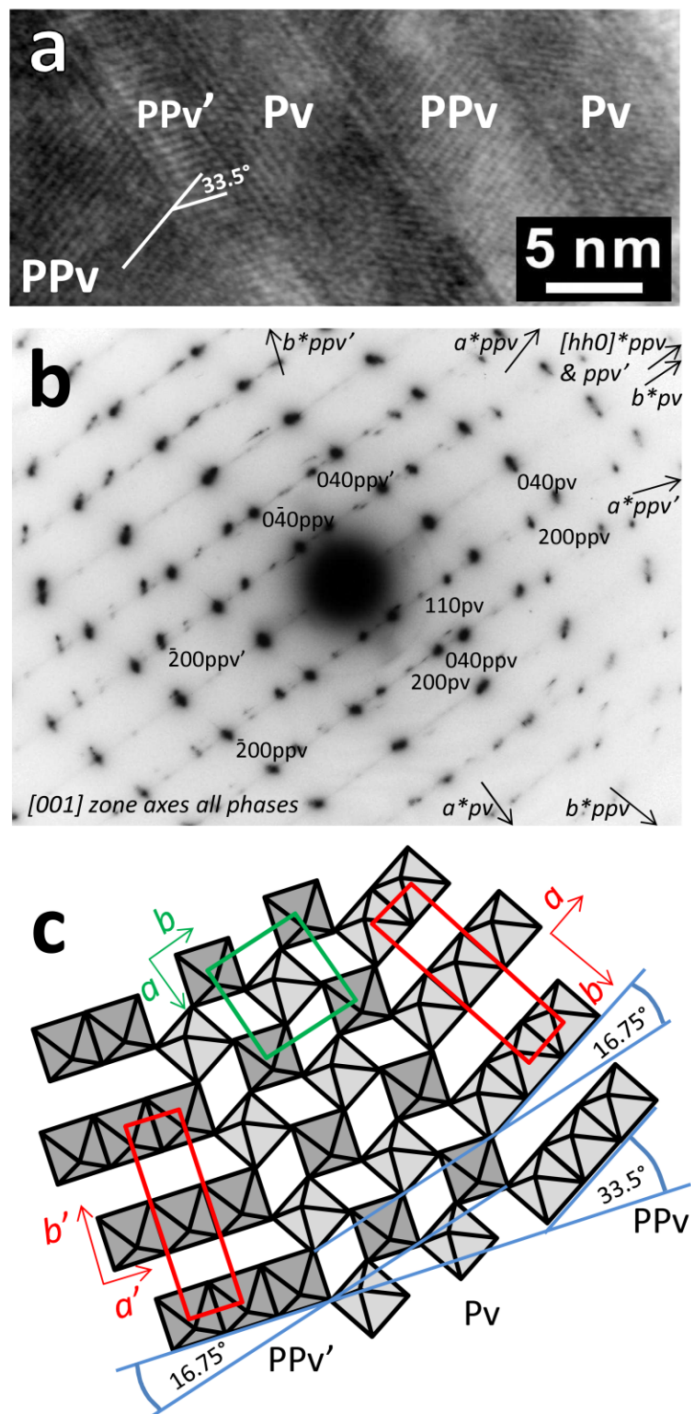


Figure 1. Transmission electron micrograph of partially-transformed NaNiF₃ perovskite.

a) High-resolution TEM image: Perovskite (Pv) and post-perovskite (PPv, PPv') domains are labelled. The spacing between the post-perovskite lattice fringes (~5 Å) is half its *b*-axis length. The 33.5° angle between the post-perovskite twin domains corresponds to the angle calculated for (110) twins using the unit cell measured by X-ray diffraction. b) Electron diffraction pattern from the area in (a). The strong mirror plane arises from the additional symmetry introduced by twinning of post-perovskite, superimposed on the perovskite symmetry. c) Sketch of NiF₆ units showing the topotactic relationships between perovskite and post-perovskite.

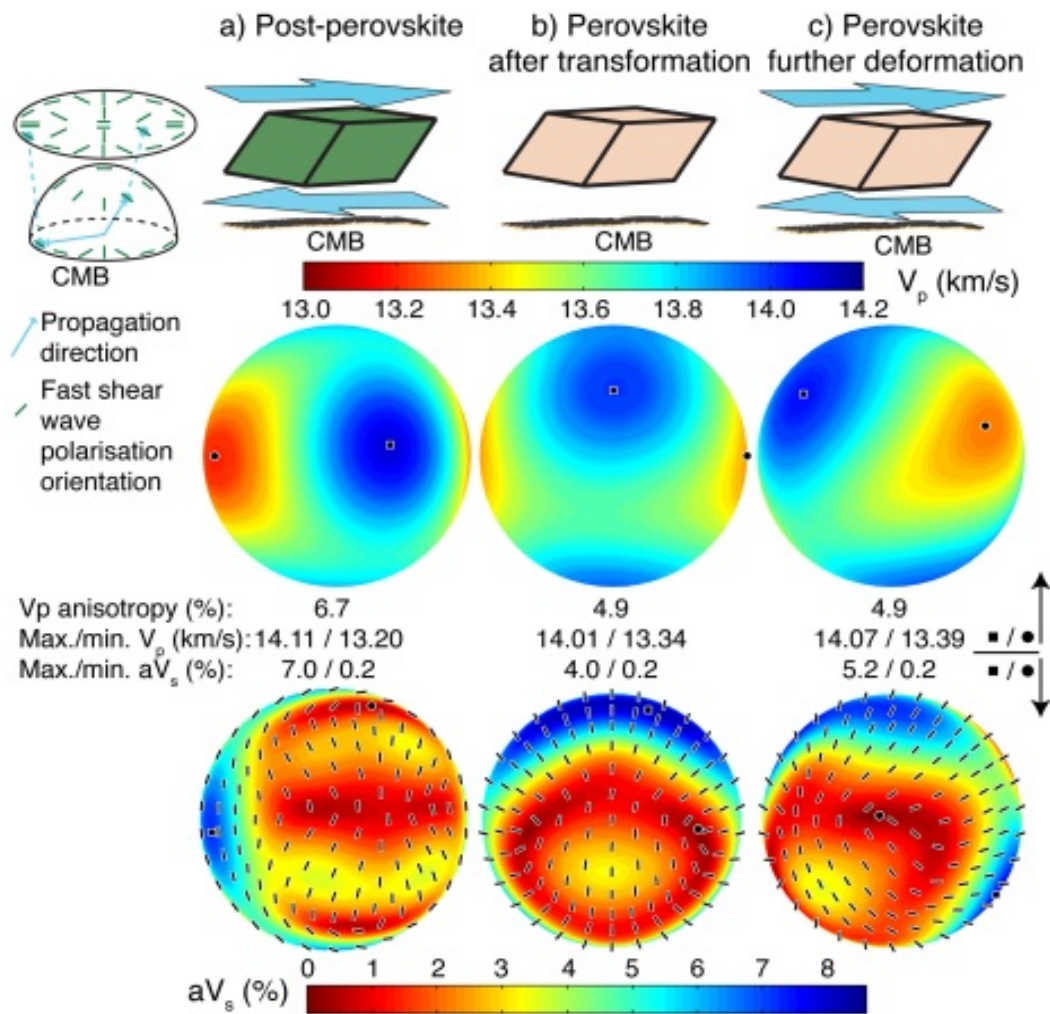


Figure 2. Seismic anisotropy predicted for the transformation from post-perovskite to perovskite. (a) post-perovskite deforming in simple shear by slip on (001) $\gamma=0.875$ (see SI); (b) perovskite transformed from post-perovskite using the observed topotaxy; (c) the perovskite texture in (b) further deformed by $\gamma=0.875$ in the perovskite stability field. The top pole figures show the P-wave velocity plotted for propagation direction. The right pole figures show the difference between the fast and slow polarised shear-waves plotted for different propagation directions; ticks show the orientation of the fast polarised shear-waves. The sense of anisotropy reverses during the transformation.